Published in final edited form as:
Oncogene. 2013 April 11; 32(15): 1888–1900. doi:10.1038/onc.2012.207.

The p44/wdr77-dependent cellular proliferation process during lung development is re-activated in lung cancer

Zhongping Gu[1,3], **Fahao Zhang**[1], **Zhi-Qiang Wang**[2], **Wencai Ma**[2], **Richard E. Davis**[2], and **Zhengxin Wang**[1,*]

[1]Department of Cancer Biology, The University of Texas MD Anderson Cancer Center, Houston, TX 77030, USA

[2]Department of Lymphoma/Myeloma, The University of Texas MD Anderson Cancer Center, Houston, TX 77030, USA

[3]Department of Thoracic Surgery, Tangdu Hospital, Fourth Military Medical University, Xi'an 710038, China

Abstract

During lung development, cells proliferate for a defined length of time before they begin to differentiate. Factors that control this proliferative process and how this growth process is related to lung cancer are currently unknown. Here, we found that the WD40-containing protein (p44/wdr77) was expressed in growing epithelial cells at the early stages of lung development. In contrast, p44/wdr77 expression was diminished in fully differentiated epithelial cells in the adult lung. Loss of *p44/wdr77* gene expression led to cell growth arrest and differentiation. Re-expression of p44/wdr77 caused terminally differentiated cells to re-enter the cell cycle. Our findings suggest that p44/wdr77 is essential and sufficient for proliferation of lung epithelial cells. P44/Wdr77 was re-expressed in lung cancer, and silencing p44/wdr77 expression strongly inhibited growth of lung adenocarcinoma cells in tissue culture and abolished growth of lung adenocarcinoma tumor xenografts in mice. The growth arrest induced by loss of *p44/wdr77* expression was partially through the p21-Rb signaling. Our results suggest that p44/wdr77 controls cellular proliferation during lung development and this growth process is re-activated during lung tumorigenesis.

Keywords

lung; lung cancer; p44/wdr77; proliferation; differentiation

Introduction

Despite advances in detection and treatment modalities, lung cancer remains the leading cause of cancer-related death worldwide [1,2]. Novel therapeutic targets for the disease are urgently needed. Such targets may include the factors that control cellular proliferation during normal lung development. The complex structure of the lung develops sequentially, first by the coordinated growth of a variety of lung cells and later by the functional

*Correspondence to: Zhengxin Wang, PhD, Department of Cancer Biology, The University of Texas MD Anderson Cancer Center, 1515 Holcombe Blvd., Houston, TX 77030, USA. Tel: 713-79-1035; Fax: 713-792-8747, zhenwang@mdanderson.org.

Author contributions: FZ performed orthotopic injection of cells and bioluminescent imaging. ZG performed the other experiments. ZQW, WM, and RED performed DNA microarray analysis. ZW wrote the manuscript.

Conflict of Interest: The authors declare no conflict of interest.

differentiation of lung epithelial cells to synthesize lipoprotein surfactants [3]. Members of the fibroblast growth factor, transforming growth factor-β, and epidermal growth factor families, as well as the secreted morphogen sonic hedgehog, appear to play important regulatory roles in lung branching morphogenesis and epithelial cell differentiation [4]. However, the factors that control cellular proliferation during lung development largely remain uncharacterized. Researchers have found that many factors that control normal lung development also play key roles in injury repair, fibrosis, and tumorigenesis in the lung [1,5].

We purified and cloned a novel androgen receptor-interacting protein, designated p44/wdr77 [6,7]. P44/WDR77 localizes in the cytoplasm of the epithelial cell at the early stage of prostate development (the growing stage) and in the adult prostate, p44/wdr77 in the nucleus establishes and maintains luminal epithelia in a growth-arrested fully differentiated state (the G1/G0 cell cycle phase) [7,8,9]. Previous studies' findings have indicated that p44/wdr77 expression may be essential for lung cell growth and lung tumorigenesis. Lu et al. [10] used microarrays to characterize the transcriptional profiles of proximal and distal regions of the murine lung at embryonic day 11.5, when branching morphogenesis is initiated. They found that the *p44/wdr77* gene was preferentially expressed in the branching regions of the murine embryonic lung, suggesting that p44/wdr77 is a modulator of cell growth in regions of branching tubules. In mice, overexpression of the transcriptional regulator Myc—the most frequently deregulated oncogene in human tumors—results in distinct types of lung adenocarcinoma. Reymann and Borlak [11] used microarray technology to identify alterations in the expression of genes based on a transgenic mouse model in which c-Myc overexpression in the alveolar epithelium resulted in the development of bronchioloalveolar carcinoma and papillary adenocarcinoma. In that study, c-Myc overexpression upregulated *p44/wdr77* gene expression, and researchers observed similar results in N-Myc loss- and gain-of-function in the murine lung [11]. Kuner et al. [12] detected p44/wdr77 expression in 58 lung tumor samples, and Wachi et al. [13] found that p44/wdr77 expression was significantly higher in lung cancer than in the normal lung cells. In addition, Gemma et al. [14] found that p44/wdr77 was highly expressed in all 29 lung cancer cell lines they examined. Taken together, these studies' findings indicate that p44/wdr77 expression may be essential for lung cell growth and lung tumorigenesis. However, despite these studies, the exact function of p44/wdr77 in lung development and in lung cancer remains unknown.

In the present study, we found that p44/wdr77 was highly expressed in mouse lung epithelial cells during the early stages of development, when cells are proliferating; however, p44/wdr77 expression was diminished in the adult lung. We also found that p44/wdr77 expression was essential and sufficient for lung epithelial cell growth and that p44/wdr77 was highly expressed in lung tumor samples and lung cancer cell lines. Silencing p44/wdr77 expression in lung adenocarcinoma cells abolished cell growth in tissue cultures and tumor xenografts in nude mice. In addition, p44/wdr77 regulated the growth of lung cancer cells partially through the p21-Rb-E2F signaling. Our findings indicate that p44/wdr77 plays an important role in the growth of lung epithelial cells and lung cancer.

Results

P44/wdr77 expression is associated with cell proliferation during lung development

Immunostaining of mouse lung tissues with an anti-p44/wdr77 antibody was performed to detect the p44/wdr77 protein. We detected p44/wdr77 protein expression in epithelial (Figure 1A, black arrows) and alveolar (white arrows) cells in the lungs from 1-, 7-, or 14-day-old mice. The level of p44/wdr77 expression decreased as mice aged; at 30 days of age, only a few epithelial cells still expressed p44/wdr77 (Figure 1A, black arrows). Co-immunostaining of p44/wdr77 with CC10 revealed that the p44/wdr77-expressing cells are

Clara cells but SP-C positive mature alveolar type II epithelial cells do not express p44/wdr77 (Supplementary Figure S1). p44/wdr77 protein expression in the lung tissue of mice older than 120 days was undetectable. Consistent with this observation, Western blot analysis revealed high levels of the expression of p44/wdr77 protein in lysates from the lungs of 1-, 7-, or 14-day-old mice (Figure 1B, lanes 1-6). The p44/wdr77 protein was weakly expressed in the lung cells of 21-, 30-, and 60-day-old mice (lanes 7-12) and not expressed in the lung cells of 120- and 390-day-old mice (lanes 13-15). These findings indicated that p44/wdr77 expression was associated with early lung development.

Staining of mouse lung tissues for the proliferation marker Ki67 (Figure 1C) revealed a significant proportion (mean ± standard error of the mean [SEM], 17%±3%) of proliferative lung cells in 1-day-old mice. We found smaller proportions of proliferative lung cells in 7-day-old mice (mean ± SEM, 15%±2%) and 14-day-old mice (mean ± SEM, 4.5%±0.5%). The proportions of proliferating epithelial cells were even lower in the lungs of 30-day-old mice (mean ± SEM, 3.1%±0.4%), 120-day-old mice (mean ± SEM, 0.7%±0.2%), and 390-day-old mice (mean ± SEM, 0.6±0.1%). These findings suggested that p44/wdr77 expression was associated with the proliferation of lung epithelial cells.

P44/wdr77 expression is sufficient to drive lung epithelial cells growth

Investigators have used a transgenic mouse strain (H-2K^{b}-tsA58) whose tissues harbor a temperature-sensitive simian virus 40 large tumor antigen (LTA), to isolate and propagate primary cells from different organs for long-term culture [15,16]. We used this mouse strain to generate primary cultures of mouse lung epithelial cells. We isolated epithelial cells from the lung and cultured them at a permissive temperature (33°C). At this temperature, the large T antigen (LTA) is expressed in lung epithelial cells (Figure 2B, lane 1, top panel), and epithelial cells are immortal. Isolated epithelial cells [lung ECs (LTA^{ts})] had high levels of expression of cytokeratine 18 (CK18), a general epithelial cell marker, and low levels of SP-C, a lung epithelial cell marker (Figure 2A). These cells grew normally at 33°C (Figure 2C, blue line) and expressed Ki67 (Figure 2D, top panel). Transferring the lung ECs (LTA^{ts}) from a permissive temperature (33°C) to a nonpermissive temperature (37°C) inactivated LTA (Figure 2B, lane 2, top panel), resulting in increased SP-C expression (Figure 2A), cell growth arrest (Figure 2C, red line), and loss of Ki67 expression (Figure 2D, middle panel). p44/wdr77 was highly expressed in lung ECs (LTA^{ts}) cultured at 33°C (Figure 2B, lane 1, middle panel); however, p44/wdr77 expression was lost in lung ECs (LTA^{ts}) cultured at 37°C (middle panel, lane 2). Lentivirus-mediated re-expression of p44/wdr77 (Figure 2B, lane 3, middle panel) relieved the arrest of these cells' growth (Figure 2C, yellow line) and proliferation (Figure 2D, bottom panel). The control lentivirus infection did not affect lung ECs (LTA^{ts}) growth at 37°C (Figure 2C, red line). Taken together, these findings suggest that p44/wdr77 was sufficient to drive the growth of quiescent lung epithelial cells.

P44/wdr77 expression is essential for lung epithelial cell growth

Immunostaining revealed that primary epithelial cells isolated from the lungs of mice carrying the floxed (*loxP*-flanked) *p44WDR77* gene locus expressed both CK18, a general epithelial cell marker, and SP-C, a lung epithelial cell–specific marker (Figure 3A). We then infected these epithelial cells with a green fluorescent protein-expressing adenovirus (control) or an adenovirus harboring Cre recombinase to delete the *p44/wdr77* gene. Western blot analysis revealed that infection with the Cre recombinase–containing adenovirus completely abolished p44/wdr77 expression in the epithelial cells (Figure 3B, lane 2 versus lane 1, top panel). The loss of the expression of the *p44/wdr77* gene completely abolished the growth (Figure 3C, red line) and proliferation (Figure 3D, middle panel) of epithelial cells and increased SP-C expression in them (Figure 3A). The re-expression of p44/wdr77 fully restored *p44*-null epithelial cell growth (Figure 3C, yellow

line) and proliferation (Figure 3D, bottom panel). These results demonstrated that p44/wdr77 was essential to lung epithelial cell growth.

P44/wdr77 expression is associated with lung tumorigenesis

Given the important role of p44/wdr77 expression in the proliferation of lung epithelial cells, we hypothesized that the expression of p44/wdr77 is de-repressed in lung cancer cells. Western blot analysis revealed that p44/wdr77 was expressed in immortalized human lung bronchial epithelial cells (Figure 4A, lane 1) and much more highly expressed in PC14P adenocarcinoma cells, A549 adenocarcinoma cells, H226 squamous cell carcinoma cells, and H69 small-cell lung carcinoma cells (Figure 4A, lanes 2-5).

We examined p44/wdr77 expression in lung tumor samples from 35 patients (15 adenocarcinomas, 15 squamous cell carcinomas, and 5 small cell lung carcinomas) and benign tissue samples from the same patients. Immunostaining experiments revealed that p44/wdr77 expression was absent from alveolar ducts as well as benign epithelium (Figure 4B, top left panels). However, strong p44/wdr77 immunostaining was present in all tumor samples but absent from the stromal cells surrounding the tumors (Figure 4B). These results indicated that expression of p44/wdr77 might have contributed to lung tumorigenesis.

Silencing p44/wdr77 expression decreases lung cancer cell growth in tissue culture

To determine whether p44/wdr77 plays a causal role in lung tumor growth, we silenced p44/wdr77 expression in lung cancer cells. Specifically, we designed short hairpin RNAs (shRNAs) targeted against 5 sequences in the coding region of the human p44/wdr77 gene and infected PC14P lung cancer cells with a lentiviral vector containing a DNA segment specifying the shRNA sequences. We also introduced a nontargeting (NT) control shRNA, whose sequence did not match that of any known human gene, into lung cancer cells. As we anticipated, Western blot analysis revealed that the control shRNA did not reduce p44/wdr77 expression (Figure 5A, lane 1). However, p44/wdr77 shRNAs 1, 2, and 3 dramatically reduced p44/wdr77 protein expression in PC14P cells 4 days after lentiviral infection (Figure 5A, lanes 2, 3, and 4 versus lane 1), and the combination of p44/wdr77 shRNAs 1 and 3 reduced p44/wdr77 protein expression by 89% compared with that of the control shRNA (lane 7 versus lane 1). The combination of p44/wdr77 shRNAs 1 and 3 also dramatically decreased p44/wdr77 protein expression in A549 and PC14GL lung cancer cells (Figure 7A, lanes 10, 13).

We plated cells expressing the NT shRNA or p44/wdr77 shRNAs in 24-well plates and counted them every day. Silencing p44/wdr77 expression with p44/wdr77 shRNA 1, 2, or 3 inhibited PC14P cell growth (Figure 5B, left panel). Silencing p44/wdr77 expression with p44/wdr77 shRNAs 1 and 3 inhibited PC14P cell growth more dramatically than silencing with p44/wdr77 shRNA 1, 2, or 3 alone did, and this inhibition was correlated with the strong ability of p44/wdr77 shRNAs 1 and 3 to individually silence p44/wdr77 expression. Silencing p44/wdr77 expression with p44/wdr77 shRNAs 1 and 3 also significantly inhibited A549 and PC14GL cell growth (Figure 5B, right panel). The expression of shRNA-resistant p44/wdr77 (Figure 5A, lane 11) restored the growth of A549 cells expressing p44/wdr77 shRNA 1 and 3 (Figure 5B, left panel, yellow line). These findings indicated that p44/wdr77 expression was required for lung adenocarcinoma cell growth in tissue culture.

P44/wdr77 expression is essential for lung adenocarcinoma cell growth in an orthotopic lung cancer model

To determine the effects of p44/wdr77 silencing on lung cancer, we observed the growth of orthotopic tumors in mice formed from PC14P and PC14GL cells expressing NT shRNA or

p44/wdr77 shRNAs. Bioluminescent imaging revealed that tumors developed in all mice (n=6) 5 weeks after we injected them with the NT shRNA–expressing PC14GL cells (Figure 6A, B). However, no tumors developed in the mice (n=6) that we injected with PC14GL cells expressing p44/wdr77 shRNAs. Mice injected with cells expressing NT shRNA had large, macroscopically visible lung tumors, whereas those injected with cells expressing p44/wdr77 shRNA did not (Figure 6C, D). These results suggested that loss of p44/wdr77 expression abolished lung adenocarcinoma tumor formation.

To exclude the possibility that the observed inhibitory effect of lung tumors by p44/wdr77 silencing was specific to PC14 lung adenocarcinoma tumor cells, we also examined orthotopic lung tumor growth in mice injected with NT shRNA- or p44 shRNA-expressing A549 lung adenocarcinoma cancer cells. Large, macroscopically visible tumors were found in the lungs of mice (n=13) 21 days after we injected them with NT shRNA–expressing A549 cells. However, no tumors were detected in the lungs of mice (n=8) injected with p44/wdr77 shRNA-expressing A549 cells. We found many macroscopically visible tumors in the lungs of mice (n=6) 45 days after injecting them with NT shRNA–expressing A549 cells but no visible tumors in the lungs of mice (n=6) injected with p44/wdr77 shRNA–expressing cells. The average weight of the lungs of the mice injected with NT shRNA–expressing A549 cells (361 mg) was higher than that of the lungs of mice injected with p44/wdr77 shRNA–expressing A549 cells (233 mg; Figure 7B), indicating the presence of massive tumors in the lungs of mice injected with control A5489 cells. H&E staining revealed a few microscopic tumors in the lungs of mice (n=6) 45 days after the injection of p44/wdr77 shRNA-expressing A549 cells (Figure 7A, left panel).

Immunostaining revealed that p44/wdr77 expression was high in A549 cells (Figure 7C, left panel), dramatically decreased by p44/wdr77 shRNA expression (middle panel), and restored by shRNA-resistant p44/wdr77 expression (right panel). The presence of microscopic tumors in the lungs of mice injected with p44/wdr77 shRNA–expressing cells may have been caused by the shRNA's incomplete suppression of p44/wdr77 expression because of variable numbers of integrated shRNA-expressing proviral vectors generated by lentiviral infection in individual cells. Therefore, we analyzed the expression of p44/wdr77 in p44/wdr77 shRNA- and NT shRNA-expressing tumors. The levels of protein expression in p44/wdr77 shRNA–expressing lung tumors and NT shRNA–expressing lung tumors were similar (Figure 7D). These findings suggested that the incomplete suppression of p44/wdr77 expression by shRNAs in a small subset of p44/wdr77 shRNA–expressing A549 cells accounted for the ability of those cells to form lung tumors.

Loss of p44/wdr77 expression leads to cell cycle arrest at the G1 phase

Flow cytometry analysis revealed no difference in the degree of apoptosis between cells expressing NT shRNA and cells expressing p44/wdr77 shRNA, indicating that the loss of p44/wdr77 expression did not induce apoptosis in lung cancer cells.

We used a BrdU incorporation assay to measure the proliferation of lung cancer A549 cells. The percentages of BrdU-positive control lung cancer cells (mean ± SEM, 82%±6%) were higher than those of p44/wdr77 shRNA–expressing lung cancer cells (mean ± SEM, 15% ±1.2%), indicating that the downregulation of p44/wdr77 expression inhibited the proliferation of lung cancer cells.

We next sought to determine whether loss of p44/wdr77 expression affected cell cycle progression in lung epithelial and lung cancer cells. Flow cytometry analysis of propidium iodide–stained cells revealed that the proportions of p44/wdr77 shRNA–expressing lung cancer cells and *p44*-null lung epithelial cells in the G1 phase were significantly higher than that of the control cells (Table 1). The proportion of p44/wdr77 shRNA–expressing cells in

the G1 phase was more than 24% higher than the proportion of control cells in the G1 phase, and the proportion of p44/wdr77 cells in the S phase was lower than the proportion of control cells in the S phase. Thus, the slow growth of p44/wdr77 shRNA–expressing cells and *p44*-null lung epithelial cells may be attributed to the arrest of cell cycle at the G1 phase. Consistent with these findings, DNA microarray expression profiling analysis revealed that the expression of genes whose function is involved in cell cycle progression was downregulated in the p44 shRNA– expressing cells (Supplementary Figure S5).

We also sought to identify the potential mechanisms by which silencing of p44/wdr77 expression caused the growth of cells to be arrested at the G1 phase. Functional proteomic analysis of NT shRNA– and p44/wdr77 shRNA–expressing A549 cells revealed that silencing of p44/wdr77 expression increased p21 expression (Supplementary Figure S2). Silencing p44/wdr77 expression also increased the expression of p21 mRNA and protein in A549 and PC14P cells (Figure 8A, lane 2; Supplementary Figure S3, S4) and in developing lung tissue samples from mice (Supplementary Figure S3). p44/wdr77 shRNA induced Rb mRNA expression (Supplementary Figure S3) but not Rb protein expression (Figure 8A, top panel, lanes 4 and 5) in A549 cells. Silencing of p44/wdr77 reduced the phosphorylation of Rb at amino acid residues 807, 811, and 795 (Figure 8A, lanes 4, 5). Expression of the p21 gene can be induced under many conditions that inhibit cell growth via cell-cycle arrest at the G1 phase, and overexpression of p21 induces cell-cycle arrest [17,18,19,20]. The Rb protein is a tumor suppressor and plays a pivotal role in the negative control of the cell cycle and in tumor progression. One of the major activities of Rb in undifferentiated cells is negative regulation of the E2F family of transcriptional factors, which prefers to activate S-phase genes [21]. Rb protein is responsible for a major G1 checkpoint at which Rb can interact with E2F proteins to block cells from entering the S phase and thus inhibit cell growth. The phosphorylation of Rb abolishes its interaction with E2F proteins, thereby relieving its inhibitory effect on cell-cycle progression. Rb overexpression induces cell-cycle arrest [22,23,24]. Consistent with these results, DNA microarray expression profiling analysis revealed that the expression of the E2F1 target genes was downregulated in p44 shRNA–expressing A549 cells (Supplementary Figure S6).

To determine whether p21 or/and Rb were responsible for the cell growth inhibition mediated by the silencing of p44/wdr77 expression, we designed shRNAs to silence the expression of p21 (8A, lane 3) and Rb (Figure 8A, lane 7) in A549 cells. Silencing the expression of p21 or/and Rb partially abolished the growth inhibition induced by p44/wdr77 silencing in A549 cells (Figure 8B). p21 overexpression–induced inhibition of A549 cell growth did not reach the level achieved by silencing p44/wdr77 expression (Figure 8C). Thus, one mechanism by which the silencing of p44/wdr77 induces cell cycle arrest is through the induction of p21 expression followed by the inhibition of Rb phosphorylation and E2F-dependent transcription.

Discussion

We found that p44/wdr77 expression is essential for the growth of lung epithelial cells and orthotopic lung adenocarcinoma tumors. Loss of p44/wdr77 expression in lung epithelial cells and lung adenocarcinoma cancer cells led to G1 cell cycle arrest via the p21-Rb-E2F signaling pathway. Our findings suggest an important role of p44/wdr77 in lung development and tumorigenesis.

P44/wdr77 is essential for growth of lung epithelial cells

The results of the present study suggest that p44/wdr77 plays essential roles in cell proliferation in the lung. Specifically, we found that p44/wdr77 expression was associated with the proliferation of lung epithelial cells. p44/wdr77 is in abundance in lung epithelial

cells harvested from mice during the early stages of development, when cells are proliferating, and in growing immortalized temperature-sensitive lung epithelial cells [lung ECs (LTA^{ts})] lung epithelial cells. In contrast, p44/wdr77 expression was absent from adult lung epithelial cells and immortalized growth-arrested lung ECs (LTA^{ts}). In addition, we found that p44/wdr77 expression was sufficient to promote the proliferation of immortalized growth-arrested lung ECs (LTA^{ts}) at a nonpermissive temperature. Finally, we found that deletion of the *p44/wdr77* gene abolished the growth of murine lung epithelial cells. These results are strong evidence that p44/wdr77 is essential and sufficient for the growth of lung epithelial cells.

During the development of a multicellular organism, cells proliferate for a defined length of time before they begin to differentiate functionally [25,26,27]. Terminal cell division must be precisely regulated to ensure that the proper numbers of differentiated cells are produced at the appropriate times. Although the control of proliferation and differentiation is highly coordinated, certain differentiation decisions are not compatible with continued proliferation. P44/WDR77 would play an essential role in these processes.

The presence of p44/wdr77 in the cytoplasm of prostate epithelial cells is required for their proliferation during the early stages of prostate development [8]. In contrast to the role of p44/wdr77 in the lung, p44/wdr77 is expressed in epithelial cells in the adult prostate and localizes in the nucleus as an androgen receptor cofactor to drive the differentiation of prostate epithelial cells [7,8]. In the present study, we found that loss of p44/wdr77 expression enhanced SP-C expression in lung epithelial cells and led to the differentiation of lung epithelial cells, which suggests that loss of p44/wdr77 expression is essential to the differentiation of epithelial cells during lung development. Loss of p44/wdr77 expression also caused significant cell enlargement (Supplementary Figure S7).

P44/wdr77 is essential for cell cycle progression through the G1 phase

We also found that p44/wdr77 was essential for lung epithelial cells to progress through the G1 phase. The process of differentiation of primitive cells into more specialized cells involves an increasing restriction in proliferation capacity, culminating in cell-cycle exit. Maintenance of cell-cycle arrest in terminally differentiated cells is important for the ultimate architecture and function of specific tissues. Whether a cell will differentiate into one or another cell type is usually determined at the G1 phase of the cell cycle. Consistent with these studies, loss of p44/wdr77 expression inhibited the proliferation of lung epithelial cells and lung adenocarcinoma (A549 and PC14P) cells via arrest at the G1 phase.

p44/wdr77 modulates the expression of key cell-cycle regulators to regulate cell-cycle progression. The loss of p44/wdr77 expression increased p21 expression in lung epithelial cells and lung adenocarcinoma cells. p21 is best known for its importance to several processes requiring cell-cycle arrest, particularly in cells with DNA damage caused by genotoxic agents [28]. P21 may also be important to the maintenance of cell-cycle arrest in differentiated cells [29,30]. The forced expression of p21 and p16 is sufficient to promote cell-cycle withdrawal and the expression of certain differentiation markers [31,32]. Conversely, the overexpression of cyclin D1 or E2F1 inhibits cell-cycle exit and cell differentiation [31,33,34]. Lens fiber cell differentiation is severely impaired in mice that are p27- and p57-deficient [35], and investigators have observed failure of myogenesis in p21 and p57 double-null mice [36]. Taken together, these results suggest that p21 expression–induced cell-cycle exit is required for differentiations.

The regulated transcription of genes required for cell-cycle progression provides an additional level of cell proliferation control. E2F transcriptional factors play a major role in the regulation of this gene transcription. The expression of E2F-regulated genes is generally

increased during late G1 and/or in S phase of the cell cycle. Rb and its family members p107 and p130 are believed to ensure cell-cycle exit and prevent cells from re-entering the cell cycle mainly by binding to E2F transcription factors, inhibiting the expression of E2F target genes, and remodeling chromatin into an inactive state [37,38,39]. In the presence of mitogens, cyclin-Cdk complexes phosphorylate Rb family members, relieving the inhibition of E2F targets and enabling S-phase entry. The compromised ability of cells with mutations in the Rb pathway to be arrested at the G1 phase is thought to be the major basis for its tumor suppressor activity [40]. In the present study, loss of p44/wdr77 expression decreased the phosphorylation of Rb and led to the activation of Rb. Activation of DNA synthesis by the adenovirus E1A in differentiated muscle cells is not simply based on targeting of Rb; E1A also has to bind to and inactivate p21, indicating that both p21 and Rb are required to prevent S-phase re-entry in these cells [41]. In proliferating cells, p21 preferentially inhibits cyclin-dependent kinases that are involved in promoting cells into S phase and in augmenting the phosphorylation of Rb protein [42]. Rb functions downstream of p21, and the activities of these two proteins in sustaining their postmitotic states may be linked [41]. Our finding that p44/wdr77 regulated cell-cycle progression via p21 and Rb does not exclude the possibility that p44/wdr77 activates additional cellular functions during lung development and lung tumorigenesis.

P44/wdr77 is required for growth of lung cancer

Our findings suggest that p44/wdr77 plays an important role in lung cancer. Tumor cells do not differentiate normally and have an unlimited capacity to proliferate. p44/wdr77 likely exerts the same biological activities during tumorigenesis as it does during normal lung development. We detected the re-expression of p44/wdr77 in lung cancer samples, which suggests that p44/wdr77 has an important role in the proliferation of lung cancer cells. Indeed, p44/wdr77 silencing dramatically inhibited lung adenocarcinoma cell growth in tissue culture and abolished the growth of lung adenocarcinoma xenografts in nude mice. Thus, p44/wdr77 expression is also essential for lung adenocarcinoma growth.

The molecular events that cause terminally differentiated lung epithelial cells to re-enter the cell cycle remain unidentified; however, our findings suggest that the re-expression of p44/wdr77 is essential to this process. These cells are susceptible to genetic mutations that lead to lung cancer. Our findings also suggest that p44/wdr77 expression and its downstream effectors are novel targets for the prevention and treatment of lung cancer. However, the ways in which this developmental program is reactivated in lung cancer cells remains unknown. Our current work is focused on the regulatory networks controlling p44/wdr77 expression during lung development, which may give us some clues about lung tumorigenesis. Current analyses using two lung adenocarcinoma cell lines (A549 and PC14P) suggest that p44/wdr77 contributes to lung adenocarcinoma development. Further studies are needed to investigate whether p44/wdr77 also contributes to the development of other subtypes of lung cancers.

Materials and methods

Lung tumor samples and immunohistochemical analysis of p44/wdr77 expression

Lung tumor samples obtained from patients who underwent surgery at Tangdu Hospital (Xi'an, China), and the study protocol was approved by its institutional review board. Samples were fixed with 10% formalin for 24 h and then embedded in paraffin. Paraffin-embedded lung tissue sections (4 μm) were stained with H&E and used for histological analysis. Lung sections were blocked with 1% fish gel and incubated with a rabbit polyclonal anti-p44/wdr77 antibody (1:1,000) overnight at 4°C. A streptavidin-biotin peroxidase detection system for use with prostate tissues (DAKO A/S, Grostrup, Denmark)

was used according to the manufacturer's instructions; 3,3′-Diaminobenzidine was used as the substrate. The primary antibody was omitted in the negative controls.

Cell culture and cell growth assay

A549, PC14P, and PC14GL cells were cultured in RPMI 1640 medium (Cellgro) with 10% (v/v) fetal bovine serum (HyClone). PC14GL cells express luciferase and were derived from PC14P cells. For a cell growth assay, cells were plated on 24-well plates (5,000 cells/well) and counted every day. For a BrdU incorporation assay, cells (50–70% confluent) were placed on coverslips and cultured with 10 μM BrdU (Sigma-Aldrich, St. Louis, MO) for 4 hrs. The BrdU-labeled cells were detected using staining with a monoclonal anti-BrdU antibody (BD, Franklin Lakes, NJ).

Orthotopic tumors

Lung cancer cells were maintained in RPMI 1640 medium containing 10% fetal bovine serum. Cells in the exponential phase of growth were harvested via treatment with a 0.25% trypsin– 0.025 ethylenediaminetetraacetic acid solution for 1 min, and the resulting cell suspension was gently agitated to produce a single-cell suspension. Cells exhibiting more than 95% viability as ascertained using trypan blue staining were used for injections. Cells were washed with Hank's balanced salt solution and resuspended in Hank's balanced salt solution diluted with an equal volume of growth factor-reduced Matrigel (Becton Dickinson). Cell suspensions were kept on ice until injection.

Six-week-old nude mice were purchased from the National Cancer Institute and maintained in a barred animal facility. An intraperitoneal injection of sodium pentobarbital (50 mg/kg) was used to anesthetize the mice prior to lung tumor cell injection. Cells (1×10^6/50 μl) were then injected into the left lateral thorax at the lateral dorsal axillary line using a 30-gauge needle. After the tumor cell injection, the mice were turned to the left lateral decubitus position and observed for 45–60 min until they recovered fully. Mice injected with PC14P or PC14GL cells were sacrificed 35 days after tumor cell injection, and mice injected with A549 cells were killed 21 or 45 days after tumor cell injection. The lungs of the mice were then removed, evaluated for tumors, and fixed with formaldehyde. Mice were handled in accordance with the guidelines published in the National Institutes of Health Guide for the Care and Use of Laboratory Animals. The MD Anderson Institutional Animal Care and Use Committee approved all the experimental procedures used for mice.

Bioluminescent imaging

Bioluminescent imaging of lung tumors was conducted using a cryogenically cooled imaging system coupled with a data acquisition computer running the LivingImage software program (Xenogen Corp., Alameda, CA). Before imaging, animals were anesthetized with a 1.5% isoflurane/air mixture in an acrylic chamber and injected intraperitoneally with 40 mg/ml luciferin potassium salt in phosphate-buffered saline (PBS) at a dose of 150 mg/kg body weight. A digital grayscale animal image was acquired, followed by the acquisition and overlay of a pseudocolor image representing the spatial distribution of detected photons emerging from active luciferase within each animal. Signal intensity was quantified as the sum of all detected photons within the region of interest per second. After the final tumor imaging study, the mice were sacrificed, and normal lung and lung tumor tissues were resected and fixed with formaldehyde. The resected tumors were histologically evaluated to verify the accuracy of the bioluminescent imaging data. Mice were handled in accordance with the guidelines published in the National Institutes of Health Guide for the Care and Use of Laboratory Animals. The MD Anderson Institutional Animal Care and Use Committee approved all the experimental procedures used for mice.

Real-time polymerase chain reaction

Total RNAs were isolated from cultured cells using TRIzol reagent and reverse transcribed into cDNA using the Reaction Ready First Strand cDNA Synthesis Kit (SuperArray Bioscience Corp.). The cDNA products were polymerase chain reaction-amplified with the RT^2 Real-Time SYBR Green PCR master mix and the gene-specific primer sets for human and murine p21, Rb, and P-actin genes (SuperArray Bioscience Corp.) using a SmartCycler II (Cepheid; 40 cycles of 30 s at 94°C, 20 s at 55°C, and 30 s at 72°C). The SmartCycler software program (version 2.0C) was used to process and quantify raw data. The 2-ΔΔCT method was used to relatively quantify target gene expression as described previously [43]. The fold change in gene expression equaled the relative quantification of expression level in the p44/wdr77 shRNA group divided by the relative quantification in the NT shRNA group.

RNA interference

P44/WDR77 shRNA(target sequence 1: 5′-GGGAACTAGATGAGAATGA-3′; target sequence 3: 5′-GTGGACACCAAGAGTACAA-3′), p21 shRNA (target sequence: 5′-AATAATTAAGACACACAAA-3′), Rb shRNA (target sequence: 5′-TGTAAGATCTCCAAAGAAA -3′), and an NT shRNA (target sequence: 5′-TTCTCCGAACGTGTCACGT-3′) were designed with a hairpin and sticky ends (ClaI and MluI). The oligonucleotides were annealed into pLVTHM, the lentiviral gene transfer vector using the ClaI and MluI restriction enzyme sites. The DNA was sequenced to determine the proper insertion points and insert lengths. The lentivirus was then produced by transfecting 293T human embryonic kidney cells (Invitrogen) with the sequence-verified PLVTHM vector, the packaging plasmid (MD2G), and the envelope plasmid (PAX2) required for viral production. Three days after transfection, the viral supernatant was collected and filtered to remove cellular debris. A549, PC14P, or PC14GL cells were plated at 60% confluence in 6-well plates and transduced with the lentivirus. After 16 h, the virus-containing medium was removed and replaced with a normal growth medium. Three days after infection, cells were split at 1:6 and allowed to grow for 3 days. Whole-cell lysates (20 mg of protein) from the infected cells were subjected to Western blot analysis, and the mRNAs isolated from the infected cells were subjected to real-time polymerase chain reaction.

Nontargetable p44/wdr77 expression

The nucleotide sequences targeted by p44/wdr77 shRNAs 1 and 3 were mutated using an oligo-directed mutagenesis kit to create a nontargetable p44/wdr77 expression vector. The target sequences GGGAACTAGATGAGAATGA and GTGGACACCAAGAGTACAA of p44/wdr77 were mutated to GGGAAtTgGAtGAGAATGA and GTGGACACCAAatcaACAA. The mutant p44/wdr77 cDNA was subcloned into a lentiviral expression vector. This recombinant lentivirus was produced with 293T cells as described above. To restore p44/wdr77 expression, p44/wdr77 shRNA– or NT shRNA–expressing A549 cells were plated in 6-well plates and transduced with a lentivirus containing either the nontargetable p44/wdr77 expression vector or an empty vector. The cells were replated after 48 h, and p44/wdr77 expression was confirmed using Western blot analysis.

Mouse lung preparation

C57BL6/J mice (n=30) were sacrificed at the age of 1, 7, 14, 30, 120, or 390 days, and their lungs were dissected. Half of each lung was used to make protein extracts and total RNA, and the other half was fixed by immersion in 4% paraformaldehyde in PBS for 60 min. The fixed lung tissues were then embedded in paraffin, and 4-μm sections were cut and mounted on Superfrost Plus adhesion slides (Fisher, Pittsburgh, PA) for H&E and immunohistochemical staining. Mice were handled in accordance with the guidelines published in the National Institutes of Health Guide for the Care and Use of Laboratory

Animals. The MD Anderson Institutional Animal Care and Use Committee approved all the experimental procedures used for mice.

Western blot analysis

p44/wdr77, p21, and Rb were detected in total protein extracts (10 μg) from the cultured cells using 10% sodium dodecyl sulfate–polyacrylamide gel electrophoresis and then transferred to Immobilon-P transfer membranes (Millipore). The membranes were washed in Tris-buffered saline with Tween 20 (10 mM Tris-HCl, pH 8, 150 mM NaCl, 0.05% Tween 20) and blocked with 5% nonfat milk in Tris-buffered saline with Tween 20 for 1 hr. The blots were then probed overnight with primary antibodies at dilutions of 1:2,000 (anti-p44/wdr77), 1:1,000 (anti-p21 [Santa Cruz Biotechnology]), or 1:1,000 (anti-Rb, anti-p807/811-Rb, and anti-p795-Rb [Cell Signaling Technology]). The blots were then incubated with a horseradish peroxide-conjugated secondary antibody for 1.5 h. Immunoreactive proteins were detected using an enhanced chemiluminescence detection system (GE Healthcare) per the manufacturer's instructions. Protein concentrations were determined using the Bradford protein assay (Bio-Rad). The protein bands were scanned using a densitometer, and the relative intensities were quantified using the ImageJ software program (ImageJ64, National Institutes of Health).

Immunohistochemistry

Formalin-fixed, paraffin-embedded murine lung sections were deparaffinized by sequential washing with xylene, graded ethanol, and PBS. Antigens were retrieved from the sections by heating the sections plus 1× Target Retrieval Solution (Dako) in a steam cooker for 30 min. The sections were then cooled and washed with PBS. Endogenous peroxide in lung tissues was blocked with 3% hydrogen peroxidase inhibitor in PBS for 12 min. Nonspecific proteins were blocked in 5% horse serum and 1% goat serum for 20 min. Slides were incubated with an anti-p44/wdr77 (1:400) or anti-Ki67 antibody overnight at 4°C and then incubated with a peroxidase-labeled anti-rabbit antibody (1:500; Jackson ImmunoResearch) for 1 h at room temperature. Signals were detected by staining the sections with 3,3′-diaminobenzidine substrate (Phoenix Biotechnologies) for 6 min and then counterstaining the sections with Gill's hematoxylin No. 3 (Sigma) for 20 s. For double staining, slides were incubated with anti-p44/wdr77 (1:200) and anti-SP-C (1:50; Santa Cruz Biotechnology) antibodies or anti-p44/wdr77 (1:200) and anti-CC10 (1:200; Santa Cruz Biotechnology) antibodies overnight at 4°C and then incubated with Dylight 488-labeled anti-rabbit IgG (1:500; Jackson ImmunoResearch) and Cy5-labeled anti-goat IgG (1:500; Jackson ImmunoResearch) antibody for 1 h at room temperature. A fluorescence confocal microscope was used to observed p44/wdr77 and SP-C or CC10 staining.

Cultured cells were allowed to grow on chamber slides and fixed with cold methanol (–20°C) for 10 min. Nonspecific proteins were blocked with 4% fish gelatin in PBS for 20 min. The cells were incubated with the primary antibodies described above at 4°C overnight and then incubated with goat anti-rat Alexa 595 (1:500; Invitrogen) at room temperature for 1 h. The cells were then washed with PBS, counterstained with SYTOX Green (Molecular Probes) for 10 min at room temperature, and mounted in Histogel (Linaris Histogel). A fluorescence confocal microscope was used to analyze the cells directly.

Gene expression profiling

Total RNA was extracted from A549 cells using the RNAqueous kit (Ambion, Austin, TX) 4 days after infection of lentivirus expressing NT shRNA or p44/wdr77 shRNA. After confirmation of RNA quality using a Bioanalyzer 2100 instrument (Agilent), 300 ng of total RNA was amplified and biotin-labeled through an Eberwine procedure using an Illumina TotalPrep RNA Amplification kit (Ambion) and hybridized to Illumina HT12 version 4

human whole-genome arrays. Processing of bead-level data was by methods previously described [44]. Significance testing for differentially-expressed probes was by the Wilcoxon rank-sum test applied to individual processed bead values, with false-discovery rate significance values (q) determined by the method of Benjamini and Hochberg [45]. Hierarchical clustering and heat mapping used Cluster and Treeview software from Eisen et al. [46]. Gene set analysis applied gene set enrichment analysis (GSEA) [47] and the hypergeometric distribution test [48] to gene sets from mSigDB and individual literature sources.

Statistical analysis

Data are presented as the means of three or more independent experiments ± the standard error of the mean (SEM). A 2-tailed unpaired Student t-test was used to determine whether differences between control and experiment samples were statistically significant. *P* values less than 0.05 were considered statistically significant.

Supplementary Material

Refer to Web version on PubMed Central for supplementary material.

Acknowledgments

We thank Joe Munch in MD Anderson's Department of Scientific Publications for editing the manuscript and Shen Gao for performing the experiment as described in Supplementary Figure S1. This work was supported in part by the National Institutes of Health through MD Anderson's Cancer Center Support Grant CA16672, National Natural Science Foundation of China (81171922), and Key Project Research Fund of Shaanxi Provincial Science and Technology Program, China. (2008K27G01). No additional external funding for this study was received. The funding agency had no role in study design, data collection or analysis, decision to publish, or manuscript preparation.

References

1. Herbst RS, Heymach JV, Lippman SM. Lung cancer. N Engl J Med. 2008; 359:1367–1380. [PubMed: 18815398]
2. Jemal A, Bray F, Center MM, Ferlay J, Ward E, et al. Global cancer statistics. CA Cancer J Clin. 61:69–90. [PubMed: 21296855]
3. Warburton D, Schwarz M, Tefft D, Flores-Delgado G, Anderson KD, et al. The molecular basis of lung morphogenesis. Mech Dev. 2000; 92:55–81. [PubMed: 10704888]
4. Mendelson CR. Role of transcription factors in fetal lung development and surfactant protein gene expression. Annu Rev Physiol. 2000; 62:875–915. [PubMed: 10845115]
5. Shi W, Xu J, Warburton D. Development, repair and fibrosis: what is common and why it matters. Respirology. 2009; 14:656–665. [PubMed: 19659647]
6. Hosohata K, Li P, Hosohata Y, Qin J, Roeder RG, et al. Purification and identification of a novel complex which is involved in androgen receptor-dependent transcription. Mol Cell Biol. 2003; 23:7019–7029. [PubMed: 12972618]
7. Zhou L, Wu H, Lee P, Wang Z. Roles of the androgen receptor cofactor p44 in the growth of prostate epithelial cells. J Mol Endocrinol. 2006; 37:283–300. [PubMed: 17032745]
8. Gao S, Wu H, Wang F, Wang Z. Altered differentiation and proliferation of prostate epithelium in mice lacking the androgen receptor cofactor p44/WDR77. Endocrinology. 151:3941–3953. [PubMed: 20519372]
9. Peng Y, Chen F, Melamed J, Chiriboga L, Wei J, et al. Distinct nuclear and cytoplasmic functions of androgen receptor cofactor p44 and association with androgen-independent prostate cancer. Proc Natl Acad Sci U S A. 2008; 105:5236–5241. [PubMed: 18356297]

10. Lu J, Qian J, Izvolsky KI, Cardoso WV. Global analysis of genes differentially expressed in branching and non-branching regions of the mouse embryonic lung. Dev Biol. 2004; 273:418–435. [PubMed: 15328023]
11. Reymann S, Borlak J. Transcription profiling of lung adenocarcinomas of c-myc-transgenic mice: identification of the c-myc regulatory gene network. BMC Syst Biol. 2008; 2:46. [PubMed: 18498649]
12. Kuner R, Muley T, Meister M, Ruschhaupt M, Buness A, et al. Global gene expression analysis reveals specific patterns of cell junctions in non-small cell lung cancer subtypes. Lung Cancer. 2009; 63:32–38. [PubMed: 18486272]
13. Wachi S, Yoneda K, Wu R. Interactome-transcriptome analysis reveals the high centrality of genes differentially expressed in lung cancer tissues. Bioinformatics. 2005; 21:4205–4208. [PubMed: 16188928]
14. Gemma A, Li C, Sugiyama Y, Matsuda K, Seike Y, et al. Anticancer drug clustering in lung cancer based on gene expression profiles and sensitivity database. BMC Cancer. 2006; 6:174. [PubMed: 16813650]
15. Jat PS, Noble MD, Ataliotis P, Tanaka Y, Yannoutsos N, et al. Direct derivation of conditionally immortal cell lines from an H-2Kb-tsA58 transgenic mouse. Proc Natl Acad Sci U S A. 1991; 88:5096–5100. [PubMed: 1711218]
16. Langley RR, Ramirez KM, Tsan RZ, Van Arsdall M, Nilsson MB, et al. Tissue-specific microvascular endothelial cell lines from H-2K(b)-tsA58 mice for studies of angiogenesis and metastasis. Cancer Res. 2003; 63:2971–2976. [PubMed: 12782605]
17. el-Deiry WS, Tokino T, Velculescu VE, Levy DB, Parsons R, et al. WAF1, a potential mediator of p53 tumor suppression. Cell. 1993; 75:817–825. [PubMed: 8242752]
18. Harper JW, Adami GR, Wei N, Keyomarsi K, Elledge SJ. The p21 Cdk-interacting protein Cip1 is a potent inhibitor of G1 cyclin-dependent kinases. Cell. 1993; 75:805–816. [PubMed: 8242751]
19. Xiong Y, Hannon GJ, Zhang H, Casso D, Kobayashi R, et al. p21 is a universal inhibitor of cyclin kinases. Nature. 1993; 366:701–704. [PubMed: 8259214]
20. Polyak K, Lee MH, Erdjument-Bromage H, Koff A, Roberts JM, et al. Cloning of p27Kip1, a cyclin-dependent kinase inhibitor and a potential mediator of extracellular antimitogenic signals. Cell. 1994; 78:59–66. [PubMed: 8033212]
21. Dyson N. The regulation of E2F by pRB-family proteins. Genes Dev. 1998; 12:2245–2262. [PubMed: 9694791]
22. Templeton DJ, Park SH, Lanier L, Weinberg RA. Nonfunctional mutants of the retinoblastoma protein are characterized by defects in phosphorylation, viral oncoprotein association, and nuclear tethering. Proc Natl Acad Sci U S A. 1991; 88:3033–3037. [PubMed: 1826560]
23. Hinds PW, Mittnacht S, Dulic V, Arnold A, Reed SI, et al. Regulation of retinoblastoma protein functions by ectopic expression of human cyclins. Cell. 1992; 70:993–1006. [PubMed: 1388095]
24. Qin XQ, Chittenden T, Livingston DM, Kaelin WG Jr. Identification of a growth suppression domain within the retinoblastoma gene product. Genes Dev. 1992; 6:953–964. [PubMed: 1534305]
25. Conlon I, Raff M. Size control in animal development. Cell. 1999; 96:235–244. [PubMed: 9988218]
26. Conlon I, Raff M. Control and maintenance of mammalian cell size: response. BMC Cell Biol. 2004; 5:36. [PubMed: 15458578]
27. Conlon IJ, Dunn GA, Mudge AW, Raff MC. Extracellular control of cell size. Nat Cell Biol. 2001; 3:918–921. [PubMed: 11584274]
28. Sherr CJ, Roberts JM. Inhibitors of mammalian G1 cyclin-dependent kinases. Genes Dev. 1995; 9:1149–1163. [PubMed: 7758941]
29. Andres V, Walsh K. Myogenin expression, cell cycle withdrawal, and phenotypic differentiation are temporally separable events that precede cell fusion upon myogenesis. J Cell Biol. 1996; 132:657–666. [PubMed: 8647896]
30. Halevy O, Novitch BG, Spicer DB, Skapek SX, Rhee J, et al. Correlation of terminal cell cycle arrest of skeletal muscle with induction of p21 by MyoD. Science. 1995; 267:1018–1021. [PubMed: 7863327]

31. Skapek SX, Rhee J, Spicer DB, Lassar AB. Inhibition of myogenic differentiation in proliferating myoblasts by cyclin D1-dependent kinase. Science. 1995; 267:1022–1024. [PubMed: 7863328]
32. Sherr CJ, McCormick F. The RB and p53 pathways in cancer. Cancer Cell. 2002; 2:103–112. [PubMed: 12204530]
33. Chen G, Lee EY. Phenotypic differentiation without permanent cell-cycle arrest by skeletal myocytes with deregulated E2F-1. DNA Cell Biol. 1999; 18:305–314. [PubMed: 10235113]
34. Wang J, Helin K, Jin P, Nadal-Ginard B. Inhibition of in vitro myogenic differentiation by cellular transcription factor E2F1. Cell Growth Differ. 1995; 6:1299–1306. [PubMed: 8845307]
35. Zhang P, Wong C, DePinho RA, Harper JW, Elledge SJ. Cooperation between the Cdk inhibitors p27(KIP1) and p57(KIP2) in the control of tissue growth and development. Genes Dev. 1998; 12:3162–3167. [PubMed: 9784491]
36. Zhang P, Wong C, Liu D, Finegold M, Harper JW, et al. p21(CIP1) and p57(KIP2) control muscle differentiation at the myogenin step. Genes Dev. 1999; 13:213–224. [PubMed: 9925645]
37. Classon M, Harlow E. The retinoblastoma tumour suppressor in development and cancer. Nat Rev Cancer. 2002; 2:910–917. [PubMed: 12459729]
38. Cobrinik D. Pocket proteins and cell cycle control. Oncogene. 2005; 24:2796–2809. [PubMed: 15838516]
39. Gonzalo S, Blasco MA. Role of Rb family in the epigenetic definition of chromatin. Cell Cycle. 2005; 4:752–755. [PubMed: 15908781]
40. Sherr CJ. Principles of tumor suppression. Cell. 2004; 116:235–246. [PubMed: 14744434]
41. Mal A, Chattopadhyay D, Ghosh MK, Poon RY, Hunter T, et al. p21 and retinoblastoma protein control the absence of DNA replication in terminally differentiated muscle cells. J Cell Biol. 2000; 149:281–292. [PubMed: 10769022]
42. Sherr CJ. G1 phase progression: cycling on cue. Cell. 1994; 79:551–555. [PubMed: 7954821]
43. Livak KJ, Schmittgen TD. Analysis of relative gene expression data using real-time quantitative PCR and the 2(-Delta Delta C(T)) Method. Methods. 2001; 25:402–408. [PubMed: 11846609]
44. Ma W, Wang M, Wang ZQ, Sun L, Graber D, et al. Effect of Long-Term Storage in Trizol on Microarray-Based Gene Expression Profiling. Cancer Epidemiol Biomarkers Prev. 2010; 19:2445–2452. [PubMed: 20805315]
45. Benjamini Y, Hochberg Y. Controlling the false discovery rate: a practical and powerful approach to multiple testing. J Roy Stat Soc B. 1995; 57:289–300.
46. Eisen MB, Spellman PT, Brown PO, Botstein D. Cluster analysis and display of genome-wide expression patterns. Proc Natl Acad Sci U S A. 1998; 95:14863–14868. [PubMed: 9843981]
47. Subramanian A, Tamayo P, Mootha VK, Mukherjee S, Ebert BL, et al. Gene set enrichment analysis: a knowledge-based approach for interpreting genome-wide expression profiles. Proc Natl Acad Sci U S A. 2005; 102:15545–15550. [PubMed: 16199517]
48. Jakt LM, Cao L, Cheah KS, Smith DK. Assessing clusters and motifs from gene expression data. Genome Res. 2001; 11:112–123. [PubMed: 11156620]

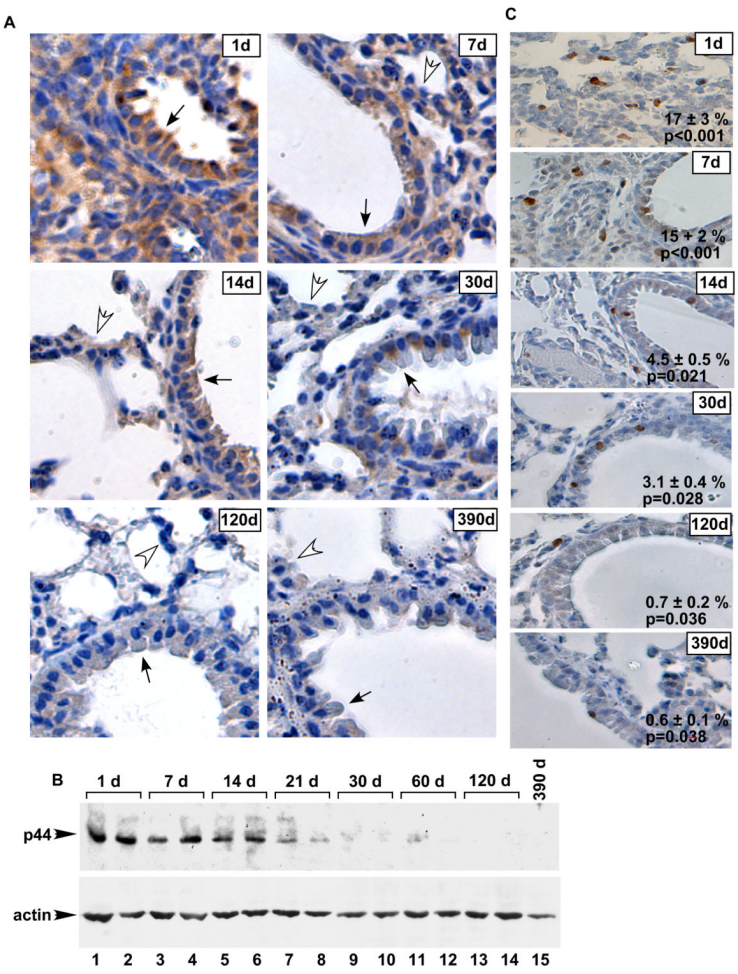

Figure 1.

p44/wdr77 expression is associated with epithelial cell proliferation during lung development in mice. (**a**) p44/wdr77 expression in lung tissue at the early stages of development. Lung tissues obtained from mice 1 (n=5), 7 (n=5), 14 (n=5), 30 (n=5), 120 (n=5), or 390 (n=3) days old were immunostained for p44/wdr77 expression. p44/wdr77-expressing cells are stained brown. Black and white arrows indicate epithelial and alveolar cells, respectively. (**b**) Western blot analysis of protein extracts from the lungs of mice 1 (n=2), 7 (n=2), 14 (n=2), 30 (n=2), 120 (n=2), or 390 (n=1) days old using an anti-p44/wdr77 antibody. Actin (bottom panel) was used as the sample loading control. (**c**) Immunostaining of the proliferation marker (antigen Ki67) in lung tissues. Ki67-positive cells are stained brown. The percentages of Ki67-positive epithelial cells are indicated.

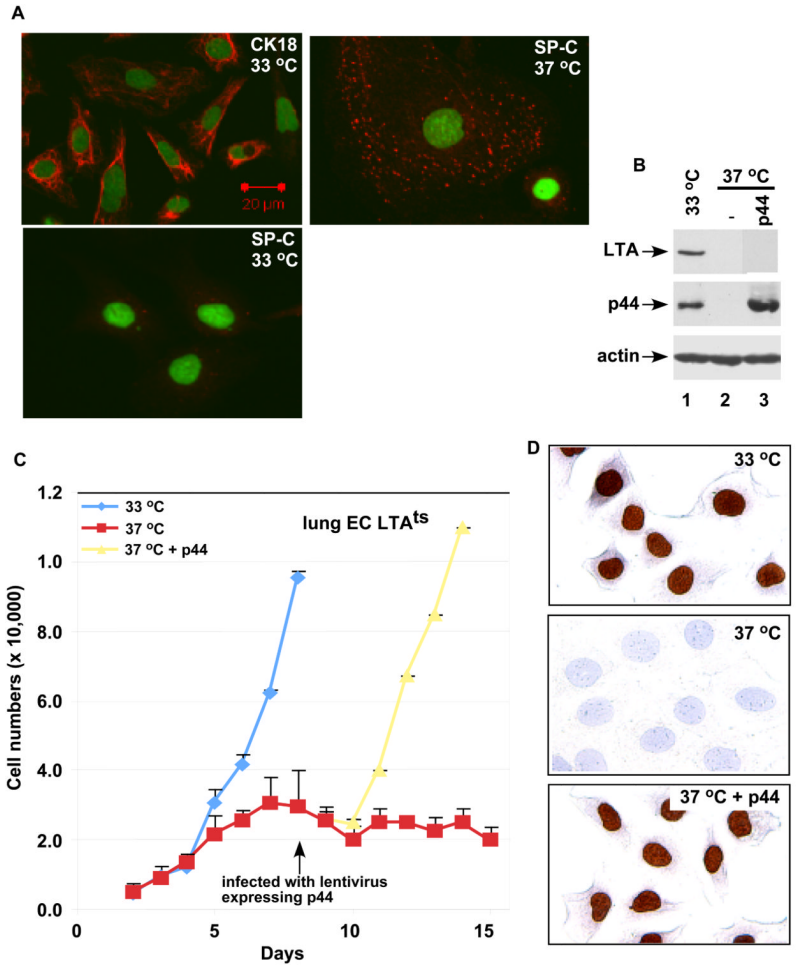

Figure 2.

p44/wdr77 is sufficient to promote lung epithelial cell growth. (**a**) LTA^{ts} lung epithelial cells [lung ECs (LTA^{ts})]expressed both CK18 and SP-C. lung ECs (LTA^{ts}) were allowed to grow at 33°C or 37°C and immunostained with an anti-CK18 or anti-SP-C antibody (red). Cell nuclei were stained with SYTOX Green. (**b**) Western blot analysis of whole cell lysates from lung ECs (LTA^{ts}) (lanes 1 and 2) or p44/wdr77-expressing lung ECs (LTA^{ts}) (lane 3) grown at 33°C (lane 1) or 37°C (lanes 2 and 3) with the indicated antibodies. (**c**) Growth curves of lung ECs (LTA^{ts}) (blue and red) and p44/wdr77-expressing lung ECs (LTA^{ts}) (yellow) at 33°C (blue) or 37°C (red and yellow). (**d**) lung ECs (LTA^{ts}) or p44/wdr77-expressing lung ECs (LTA^{ts}) were allowed to grow at 33°C or 37°C in the presence of BrdU and immunostained with an anti-BrdU antibody (blown).

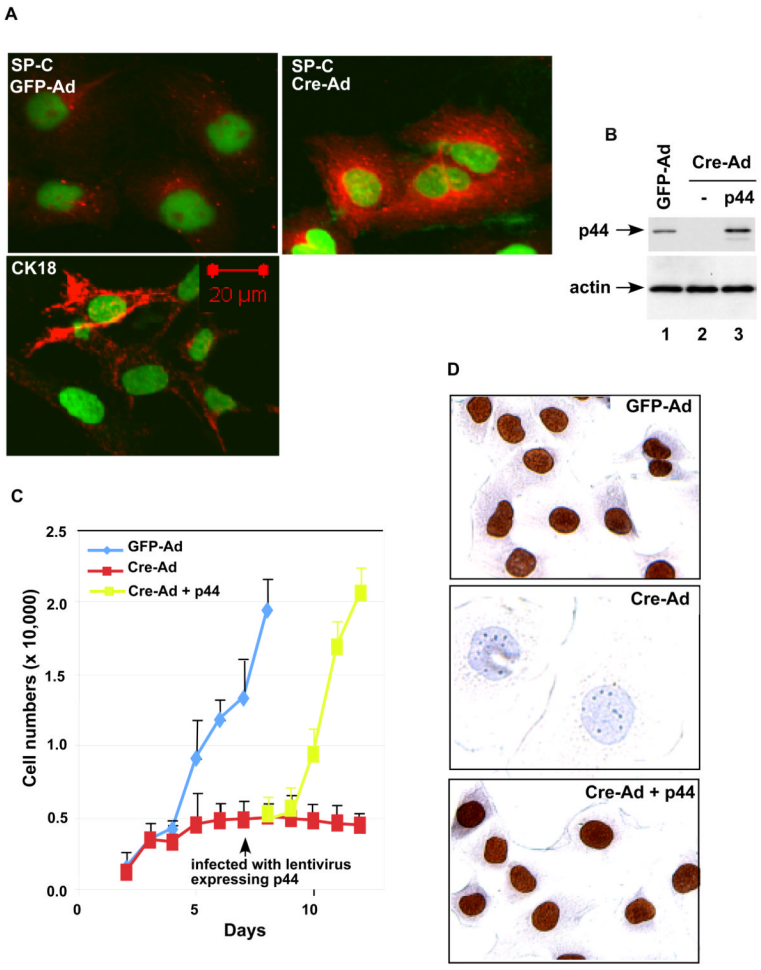

Figure 3.

p44/wdr77 is essential to lung epithelial cell growth. (**a**) Murine lung epithelial cells were immunostained with an anti-CK18 or anti-SP-C antibody (red). Cell nuclei were stained with SYTOX Green. (**b**) Cre-mediated deletion and lentivirus-mediated re-expression of p44/wdr77 in lung epithelial cells. Western blot analysis of whole cell lysates from lung epithelial cells infected with a GFP-adenovirus (GFP-Ad), Cre-adenovirus (Cre-Ad), or Cre-adenovirus plus p44-expressing lentivirus. (**c**) Growth curves of epithelial cells infected with GFP-Ad (blue), Cre-Ad (red), or Cre-Ad plus a p44/wdr77-expressing lentivirus (yellow). (**d**) Lung epithelial cells infected with GFP-Ad (top), Cre-Ad (middle), or Cre-Ad plus a p44-expressing lentivirus (bottom) were allowed to grow in the presence of BrdU and immunostained with an anti-BrdU antibody (blown).

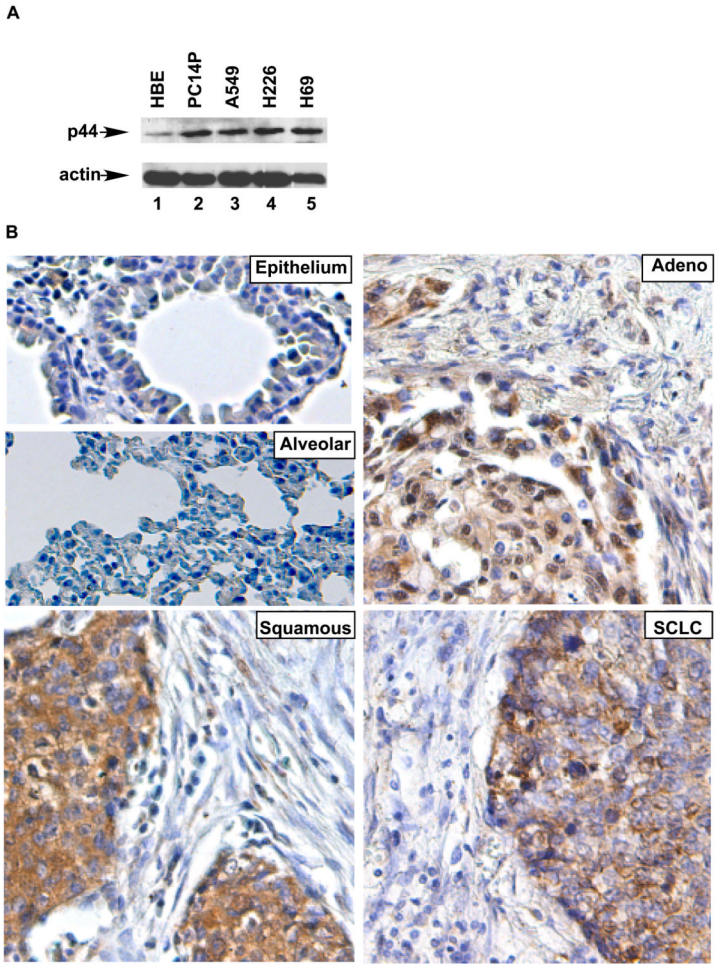

Figure 4.

p44/wdr77 expression is associated with lung cancer tumorigenesis. (**a**) Western blot analysis of p44/wdr77 expression in immortalized human lung epithelial cells (HBE) and in lung cancer cell lines (lanes 2-5). (**b**) Immunostaining for p44/wdr77 in benign lung tissues and in lung cancer samples. Adeno, adenocarcinoma; Squamous, squamous cell carcinoma; SCLC, small-cell lung carcinoma.

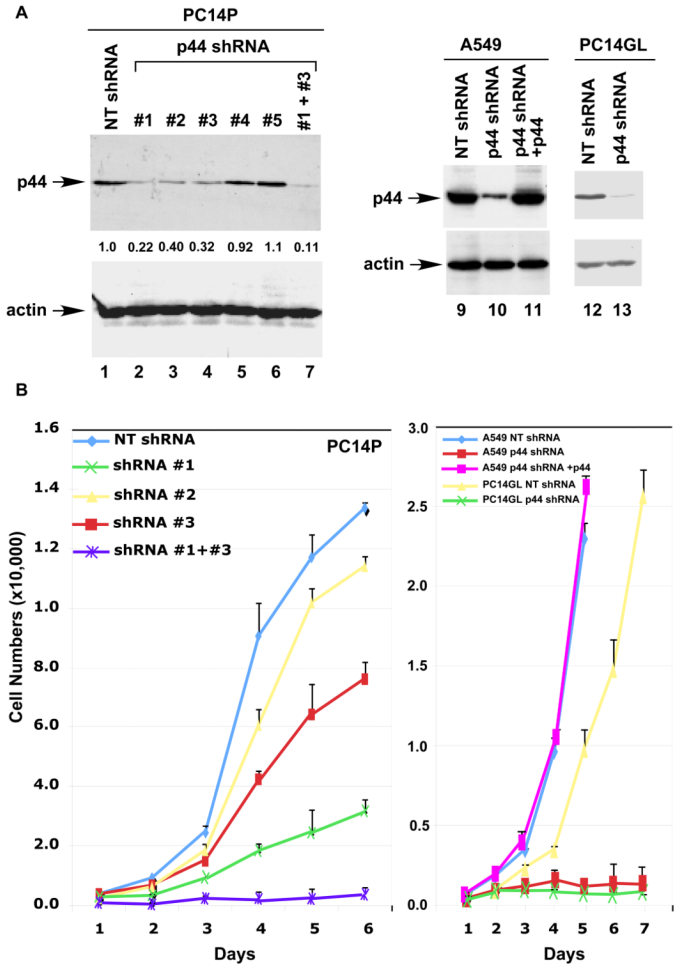

Figure 5.

Silencing of p44/wdr77 expression inhibits lung cancer cell growth. (**a**) shRNA-mediated silencing of p44/wdr77 expression in lung cancer cells. Western blot analysis of whole cell lysates from PC14P, A549, and PC14GL cells infected with a lentivirus expressing NT shRNA (lanes 1, 9, and 12) or p44/wdr77 shRNAs (lanes 2-7, 10, 11, and 13). Western blot analyses of A549 cells infected with a lentivirus expressing p44/wdr77 shRNAs 1 plus 3 or lentivirus expressing shRNA-resistant p44/wdr77 are shown in lane 11. (**b**) Growth curves of lung cancer cells expressing NT shRNA, p44/wdr77 shRNAs, or p44/wdr77 shRNA plus shRNA-resistant p44/wdr77. Differences between control and experiment samples were analyzed by unpaired Student *t-test* and the *p* values are less than 0.0001.

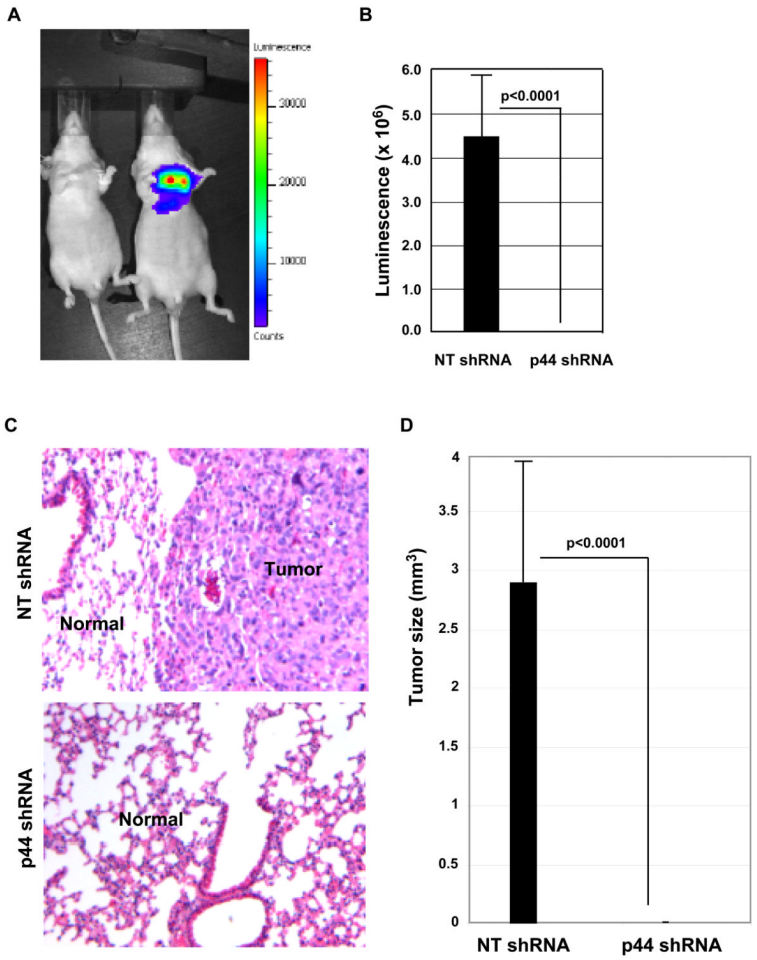

Figure 6.

Loss of p44/wdr77 expression abolished pc14p and pc14gl tumor growth. (**a**) Representative bioluminescent images of mice injected with PC14GL cells stably expressing NT shRNA (right) or p44/wdr77 shRNAs (left). (**b**) Bioluminescent imaging was used to estimate tumor volumes in the mice. Data are the means ± SEMs for 6 animals per group. (**c**) Lung tissues from mice injected with PC14P cells stably expressing NT shRNA (top) or p44/wdr77 shRNAs (bottom) stained with H&E. (**d**) Volumes of tumors in the mice developed from PC14P and PC14GL cells expressing NT shRNA or p44/wdr77 shRNA. Data are the means ± SEMs for 12 animals per group.

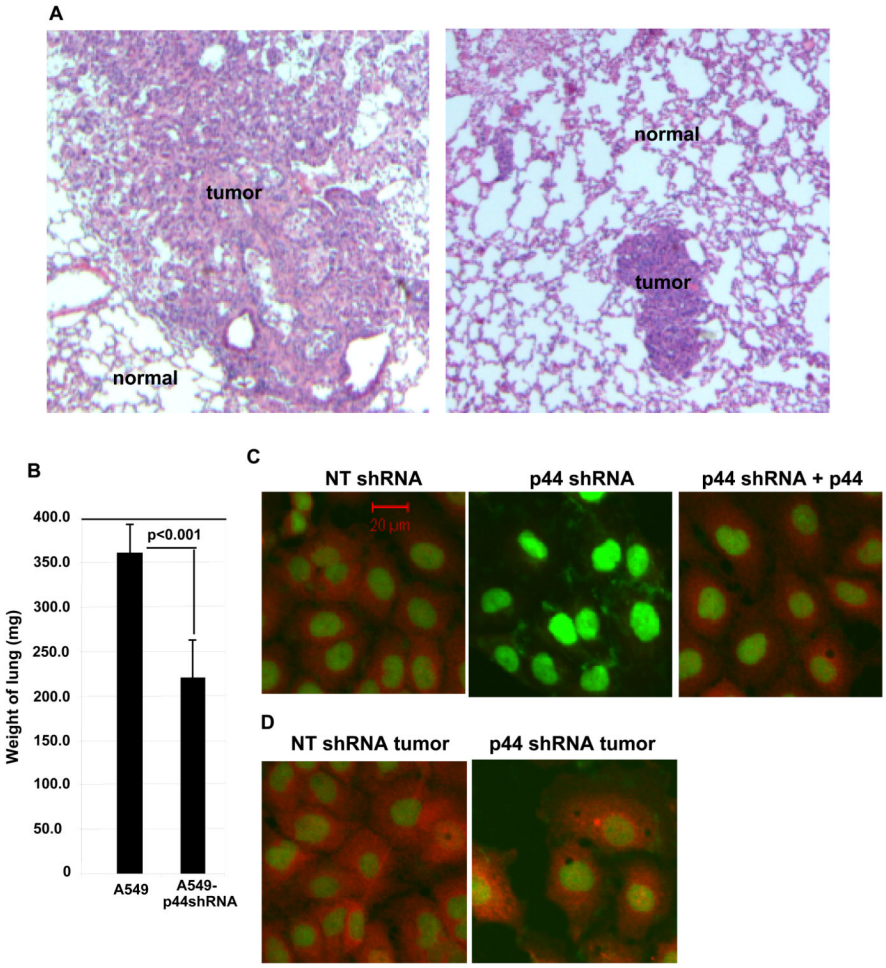

Figure 7.

Loss of p44/wdr77 expression suppressed a549 tumor growth. (**a**) Lung tissues obtained from mice injected with A549 cells stably expressing NT shRNA (left) or p44/wdr77 shRNAs (right) stained with H&E. (**b**) Weights of the lungs from mice injected with A549 cells expressing NT shRNA or p44/wdr77 shRNA. Data are the means ± SEMs for 6 animals per group. (**c**) p44/wdr77 immunostaining of A549 cells expressing NT shRNA (left), p44/wdr77 shRNA (middle), or p44/wdr77 shRNA plus p44/wdr77 (right). The nuclei were stained with SYTOX Green. (**d**) p44/wdr77 immunostaining of A549 orthotopic tumors expressing NT shRNA (left) or p44/wdr77 shRNAs (right). The nuclei were stained with SYTOX Green.

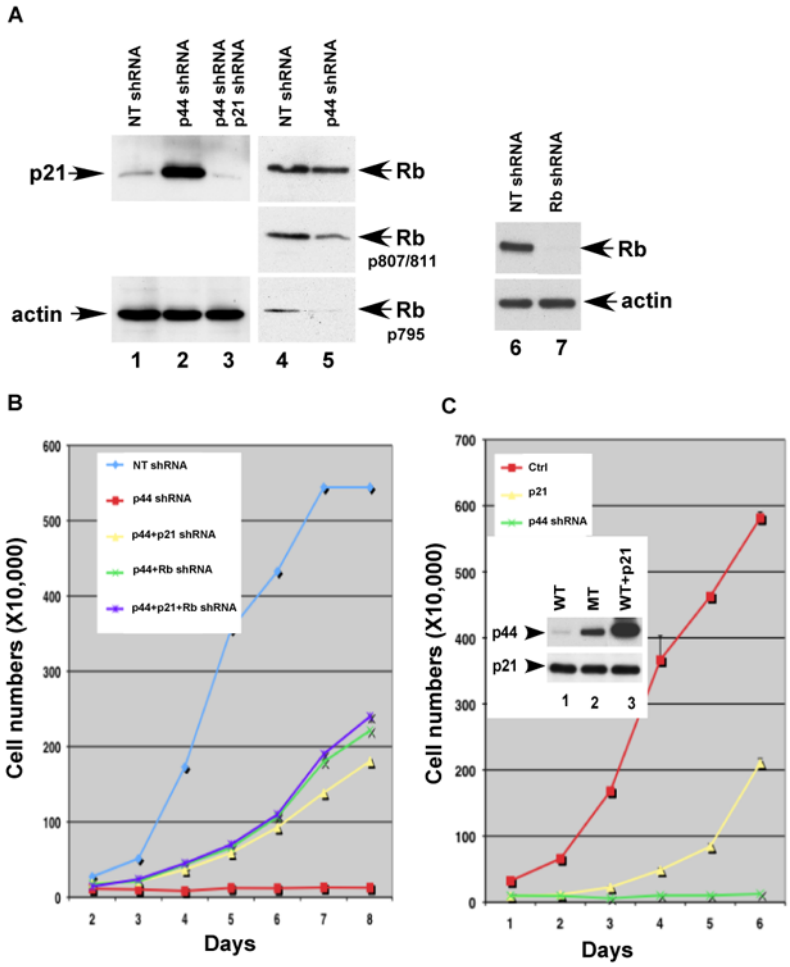

Figure 8.

p44/wdr77 targets p21-Rb signaling to control lung cancer cell growth. (**a**) Western blot analysis of whole-cell lysates derived from A549 cells expressing NT shRNA, p44/wdr77 shRNA, p44/wdr77 shRNA plus p21 shRNA, or Rb shRNA stained with anti-p21, anti-Rb, anti-Rb phospho807/811, anti-Rb phospho795, or anti-actin antibodies. (**b**) Growth curves of A549 cells infected with a lentivirus expressing p21, lentivirus expressing NT shRNA, lentivirus expressing p44 shRNA, lentivirus expressing p44 plus p21 shRNAs, lentivirus expressing p44 plus Rb shRNAs, or lentivirus expressing p44 shRNA, p21 shRNA, and Rb shRNA. Differences between control and experiment samples were analyzed by unpaired Student *t-test* and the *p* values are less than 0.0001. (**c**) Growth curves of A549 cells infected with a control lentivirus, lentivirus expressing p21, or lentivirus expressing p44 shRNA are shown. The insert shows Western blot analysis of A549 cells infected with a control lentivirus (WT), lentivirus expressing p21 (WT + p21), or lentivirus expressing p44/wdr77 shRNA (MT). Differences between control and experiment samples were analyzed by unpaired Student *t-test* and the *p* values are less than 0.0001.

Table 1

Cell cycle distribution of cells with down-regulation of p44 expression

Cells		G1 (%)	G2 (%)	S(%)	Sub G (%)
A549	NT shRNA	39.2 ±3.1	16.9 ±1.2	43.8 ± 2.5	2.2 ± 0.4
	p44 shRNA	63.9 ± 2.2	9.4 ± 0.7	26.6 ± 3.3	2.6 ±0.6
PC14P	NT shRNA	59.2 ±3.2	8.6 ±1.1	32.1 ± 2.5	2.2 ± 0.4
	p44 shRNA	86.9 ± 2.9	5.9 ±0.6	7.1 ±1.5	2.2 ± 0.5
EC (p44 flox)	GFP-Ad	38.1 ±3.1	41.2 ±2.2	20.6 ±1.5	3.8 ± 0.7
	Cre-Ad	64.5 ± 3.2	11.7 ±0.5	23.6 ± 2.3	4.8 ± 0.6